

New $\text{Bi}_2\text{Mo}_{1-x}\text{W}_x\text{O}_6$ Solid Solution: Mechanochemical Synthesis, Structural Study, and Ferroelectric Properties of the $x = 0.75$ Member

A. Castro,^{*,†} P. Bégue,^{†,§} B. Jiménez,[†] J. Ricote,[†] R. Jiménez,[†] and J. Galy[‡]

Instituto de Ciencia de Materiales de Madrid, CSIC, Cantoblanco, 28049 Madrid, Spain, and Centre d'Elaboration de Matériaux et d'Etudes Structurales, CNRS, 29 rue Jeanne Marvig, B.P. 4347, 31055 Toulouse Cedex 4, France

Received February 11, 2003. Revised Manuscript Received June 24, 2003

To search for new ferroelectric materials exhibiting an Aurivillius structural type, the syntheses of the solid solution $\text{Bi}_2\text{Mo}_{1-x}\text{W}_x\text{O}_6$ has been undertaken. A phase with a large homogeneity range exists for $0.5 < x \leq 1.0$. The thermal behavior of mechanochemically assisted precursor powders has been studied, showing that the consecutive crystallization of fluorite and Aurivillius-type phases arrives before a ferro-paraelectric transition occurs. TEM studies of the representative mechanoactivated 1:0.25:0.75 $\text{Bi}_2\text{O}_3\text{:MoO}_3\text{:WO}_3$ mixture indicates that mechanochemical synthesis of a $\text{Bi}_2\text{Mo}_{0.25}\text{W}_{0.75}\text{O}_6$ amorphous phase takes place. The ferroelectric properties of $\text{Bi}_2\text{Mo}_{0.25}\text{W}_{0.75}\text{O}_6$ well-densified ceramic material have been measured. The crystal structure of $\text{Bi}_2\text{Mo}_{0.25}\text{W}_{0.75}\text{O}_6$ has been refined using X-ray and neutron powder diffraction combined with Rietveld analysis. This oxide is isostructural with both $\gamma(\text{L})$ Bi_2MoO_6 and Bi_2WO_6 belonging to the orthorhombic system, space group $Pca2_1$, $a = 5.44547(7)$ Å, $b = 16.3731(2)$ Å, and $c = 5.46659(7)$ Å, $V = 487.40(1)$ Å³, $Z = 4$, and $\rho_{\text{cal}} = 9.21$ g·cm⁻³. The structure keeps the Aurivillius-type framework with alternating $[\text{Bi}_2\text{O}_2]$ and $[\text{Mo}/\text{WO}_4]$ layers. The structural characteristics of $\text{Bi}_2\text{Mo}_{0.25}\text{W}_{0.75}\text{O}_6$ can be considered intermediate between those of $\gamma(\text{L})$ Bi_2MoO_6 and Bi_2WO_6 .

Introduction

Bismuth molybdates have been largely studied because of their interesting catalytic properties in selective olefin oxidation and ammonoxidation processes.^{1,2} Perhaps Bi_2MoO_6 is one of the most complex compounds belonging to this system, because it crystallizes in four polymorphic phases, that can be isolated at increasing temperatures depending on the synthesis protocol, with each of them exhibiting different applications as ionic conductor,³ ferroelectric material,⁴ and also catalyst.⁵ The $\gamma(\text{F})$ phase, showing a fluorite-like structure, is a low-temperature stable phase, which can be isolated only from mechanochemically activated precursor mixture of oxides.^{6,7} The $\gamma(\text{L})$ phase is easily obtained by the traditional ceramic route, at moderate tempera-

tures, remaining stable up to 600 °C, when a reversible $\gamma(\text{L}) \leftrightarrow \gamma(\text{I})$ transition occurs. Both $\gamma(\text{L})$ and $\gamma(\text{I})$ phases show a layered Aurivillius-type structure, where infinite $[\text{Bi}_2\text{O}_2]$ and $[\text{MoO}_4]$ sheets alternate along one of the crystallographic axes. Recent electrical studies indicate that the mentioned $\gamma(\text{L}) \leftrightarrow \gamma(\text{I})$ Bi_2MoO_6 transition is related to a ferro-paraelectric type transition.⁶ Finally, these polymorphs heated at temperatures higher than 670 °C derive to the stable $\gamma(\text{H})$ phase, which remains unaltered on cooling. The $\gamma(\text{H})$ form exhibits an original structure where no $[\text{MoO}_4]$ layers are observed but MoO_4 tetrahedra surrounding columns and ribbons of Bi–O are found instead.^{8,9}

On the other hand, the analogous oxide Bi_2WO_6 has also been studied in great detail as a consequence of its promising electrical and optical properties such as ferroelectricity, piezoelectricity, pyroelectricity, and nonlinear dielectric susceptibility.^{10–14} From a structural viewpoint, this oxide is isostructural with the $\gamma(\text{L})$

* Corresponding author. Phone: (+34) 91 334 9000. Fax: (+34) 91 372 0623. E-mail: acastro@icmm.csic.es.

[†] Instituto de Ciencia de Materiales de Madrid, CSIC.

[‡] Centre d'Elaboration de Matériaux et d'Etudes Structurales, CNRS.

[§] Current address: Civil Engineering Department, Sherbrooke University, Sherbrooke, Québec, J1K 2R1, Canada.

(1) Moro-Oka, Y.; Ueda, W. *Adv. Catal.* **1994**, *40*, 233.

(2) Baptist, Ph. A.; der Kinderen, A. H. W. M.; Leeuwenburgh, Y.; Metz, F. A. M. G.; Schuit, G. C. A. *J. Catal.* **1993**, *18*, 273.

(3) Chiodelli, G.; Magistris, A.; Spinolo, G.; Tomasi, C.; Antonucci, V.; Giordano, N. *Solid State Ionics* **1994**, *74*, 37.

(4) Ismailzade, I. H.; Aliyev, I. M.; Ismailzov, R. M.; Alekberov, A. I.; Rzayev, D. A. *Ferroelectrics* **1979**, *22*, 853.

(5) Portela, M. F.; Pinheiro, C.; Dias, C.; Pires, M. J. *Stud. Surf. Sci. Catal.* **1991**, *67*, 77.

(6) Bégue, P. Ph.D. Thesis, Université Paul Sabatier, Toulouse, France, 2001.

(7) Castro, A. *Bol. Soc. Esp. Ceram. Vidr.* **2002**, *41*, 45.

(8) Buttrey, D. J.; Vogt, T.; Wilgruber, U.; Robinson, W. R. *J. Solid State Chem.* **1994**, *111*, 118.

(9) Bégue, P.; Enjalbert, R.; Galy, J.; Castro, A. *Solid State Sci.* **2000**, *2*, 637.

(10) Newkirk, H. W.; Quadflieg, P.; Liebertz, J.; Kockel, A. *Ferroelectrics* **1972**, *4*, 51.

(11) Stefanovich, S. Yu.; Venetsev, N. Yu. *Phys. Status Solidi A* **1973**, *20*, K49.

(12) Ismailzade, I. G.; Mirishli, F. A. *Kristallografiya* **1970**, *14*, 738.

(13) Yanovskii, V. K.; Voronkova, V. I.; Alexandrovskii, A. L.; D'yakov, V. A. *Dokl. Akad. Nauk SSSR* **1975**, *222*, 94.

(14) Utkin, V. I.; Roginskaya, Yu. E.; Voronkova, V. I.; Yanovskii, V. K.; Galyamov, B. Sh.; Venetsev, Yu. N. *Phys. Status Solidi A* **1980**, *59*, 75.

Bi_2MoO_6 phase^{15,16} and, as Thompson et al. have emphasized,¹⁷ the property of ferroelectricity might not be affected by the intergrowth of these two structures.

The effect of doping on various physical and chemical properties of solid materials is well-known, and this effect has been extensively exploited in piezoelectrics and ferroelectrics to improve their performance. For example, there have been several reports on the effect of doping in PZT systems^{18,19} and Bi-layered Aurivillius phases.²⁰ Following this trend, some of the authors have explored the synthesis of new solid solutions by the doping of both bismuth and molybdenum positions in Bi_2MoO_6 with similar cations, like antimony or arsenic^{9,21} and chromium,²² respectively. This has always resulted in the stabilization of the nonferroelectric $\gamma(\text{H})$ polymorph. Now, it could be expected that the substitution of W^{6+} for Mo^{6+} may stabilize the ferroelectric $\gamma(\text{L})$ polymorph, because of the structural similarities between the cations, thus leading to a new solid solution with improved properties.

This work reports on the synthesis of this new solid solution, with the general composition $\text{Bi}_2\text{Mo}_{1-x}\text{W}_x\text{O}_6$, using both solid-state and mechanochemical activation synthesis methods. The objective is to isolate single phases, and, then, obtain good ceramic materials. Moreover, a structural study and an electrical characterization of the representative $\text{Bi}_2\text{Mo}_{0.25}\text{W}_{0.75}\text{O}_6$ member have been carried out, and the results are reported and compared with the characteristics of the extreme compositions in the solid solution.

Experimental Procedure

Two different methods have been applied to synthesize $\text{Bi}_2\text{Mo}_{1-x}\text{W}_x\text{O}_6$ phases: classical solid-state reaction and mechanochemical activation. For both procedures, the mixture of Bi_2O_3 , MoO_3 , and WO_3 of analytical grade, in stoichiometric proportion to form $\text{Bi}_2\text{Mo}_{1-x}\text{W}_x\text{O}_6$ ($0 \leq x \leq 1$), was initially homogenized by hand in an agate mortar. In the traditional ceramic route, the mixture was treated at increasing temperatures from 550 to 950 °C for 12 h, with intermediate regrinding steps. For the mechanochemical activation a vibrating mill Fritsch Pulverisette 0 was used. The starting oxide mixture (10 g) was placed in a stainless steel pot with one 5-cm diam ball. The powders were milled for 30 days.

The purity of the phases was checked by X-ray diffraction using a Siemens Kristalloflex 810 generator and a D-501 goniometer equipped with a graphite monochromator. The data were recorded between 5° and 65° (2θ) at increments of 0.05° (2θ) and a counting time of 1 s per step. Additional X-ray data were collected for the refinement of the structure with the same diffractometer, at room temperature, but in this case the data were recorded between 5° and 100° (2θ) with an increment of 0.02° (2θ) and a counting time of 10 s per step. Furthermore, high-temperature patterns were recorded on a Philips PW1310 diffractometer fitted with an Anton Paar HTK

10 attachment to stabilize the temperature during measurement. The diffractograms were obtained by depositing a small quantity of powder onto a platinum sheet placed on a tantalum strip, which was the heating element. The recordings were taken from 5 to 70° (2θ) with a scan rate of 0.02° per second. The temperature was monitored by a Pt–Pt 13% Rh thermocouple welded in the center of the platinum sheet. The heating rate was 10 °C·min⁻¹ and the temperature was stabilized during 1 h. The Cu K α doublet ($\lambda = 0.15418$ nm) was used in all X-ray experiments.

Neutron data were recorded at room temperature on the powder diffractometer D1A at the Institut Laue Langevin in Grenoble. A wavelength of 1.910 Å was selected from a Ge monochromator. The pattern was recorded with increments of 0.05° (2θ) and 250 s of counting time, between 10° and 150° (2θ).

The structure was refined by the Rietveld method using the program Fullprof.²³ No regions were excluded in the refinement.

Dispersed particles of the mechanochemically activated precursor with $\text{Bi}_2\text{Mo}_{0.25}\text{W}_{0.75}\text{O}_6$ composition were characterized by transmission electron microscopy (TEM). A Philips Tecnai-20 FEG working at 200 kV and equipped with energy dispersion spectroscopy (EDS) was used.

The thermal behavior of mechanochemically activated powders was studied by thermogravimetric (TG) and differential thermal analysis (DTA). The measurements were carried out in air, from room temperature to 1000 °C on a Seiko 320 instrument at a heating/cooling rate of 10 °C·min⁻¹. About 10 mg of sample was used for each run, with Al_2O_3 as reference material.

Ceramics of $\text{Bi}_2\text{Mo}_{0.25}\text{W}_{0.75}\text{O}_6$ composition were prepared from mechanochemically activated powders by sintering at 925 °C under axial pressure of 200 kg·cm⁻². Densifications of 97–99% were reached. Dielectric measurements as a function of the temperature were performed with a HP4194A impedance analyzer. Ferroelectric hysteresis loops were traced using the electrical current integration technique with a sinusoidal wave 1 Hz in frequency and 600 V in amplitude.

Results and Discussion

The $\text{Bi}_2\text{Mo}_{1-x}\text{W}_x\text{O}_6$ Solid Solution. With the aim of verifying the possible substitution of W^{6+} for Mo^{6+} in Bi_2MoO_6 , various samples of nominal composition $\text{Bi}_2\text{Mo}_{1-x}\text{W}_x\text{O}_6$ were prepared by conventional solid-state reaction, as described in the experimental part of this paper. The X-ray powder diffraction patterns of these samples after heating at 950 °C are plotted in Figure 1. At first sight, a mixture of $\gamma(\text{H})$ Bi_2MoO_6 and Bi_2WO_6 phases is obtained for $x < 0.5$, which is easily understood taking into account that $\gamma(\text{H})$ is the stable form of Bi_2MoO_6 at high temperature, at the same time that Bi_2WO_6 Aurivillius-type phase remains stable up to 1000 °C or higher; so, for these compositions no substitution of tungsten for molybdenum seems to occur. A careful examination of the X-ray diffraction pattern of the $\text{Bi}_2\text{Mo}_{0.5}\text{W}_{0.5}\text{O}_6$ sample (Figure 2) shows that the major phase present is isostructural to Bi_2WO_6 and $\gamma(\text{L})$ Bi_2MoO_6 , although a small quantity of $\gamma(\text{H})$ type remains. Finally, for x ranging from 0.75 to 1 single phases belonging to the Bi_2WO_6 and $\gamma(\text{L})$ Bi_2MoO_6 structural type are obtained, leading to the solid solution $\text{Bi}_2\text{Mo}_{1-x}\text{W}_x\text{O}_6$ with $0.5 < x \leq 1$.

Study of $\text{Bi}_2\text{Mo}_{0.25}\text{W}_{0.75}\text{O}_6$ Phase. Considering one of the major aims of this work is to ascertain the ferroelectric character of the new $\text{Bi}_2\text{Mo}_{1-x}\text{W}_x\text{O}_6$ materi-

(15) Teller, R. G.; Brazdil, J. F.; Grasselli, R. K.; Jorgensen, J. D. *Acta Crystallogr. C* **1984**, *40*, 2001.

(16) Knight, K. S. *Mineral. Mag.* **1992**, *56*, 399.

(17) Thompson, J. G.; Schmid, S.; Withers, R. L.; Rae, A. D.; Fitzgerald, J. D. *J. Solid State Chem.* **1992**, *101*, 309.

(18) Kulcsar, F. *J. Am. Ceram. Soc.* **1959**, *42*, 343.

(19) Taquín, R. B.; Holman, R. L.; Fulrath, R. M. *J. Am. Ceram. Soc.* **1971**, *54*, 113.

(20) Durán-Martín, P.; Castro, A.; Millán, P.; Jiménez, B. *J. Mater. Res.* **1998**, *13*, 2565.

(21) Bégué, P.; Enjalbert, R.; Castro, A. *J. Solid State Chem.* **2001**, *159*, 72.

(22) Bégué, P.; Rojo, J. M.; Iglesias, J. E.; Castro, A. *J. Solid State Chem.* **2002**, *166*, 7.

(23) Rodríguez-Carbajal, J. *Fullprof, Version 0.2*; Mars 98, Laboratoire Leon Brillouin (CEA-CNRS), Saclay, France, 1998.

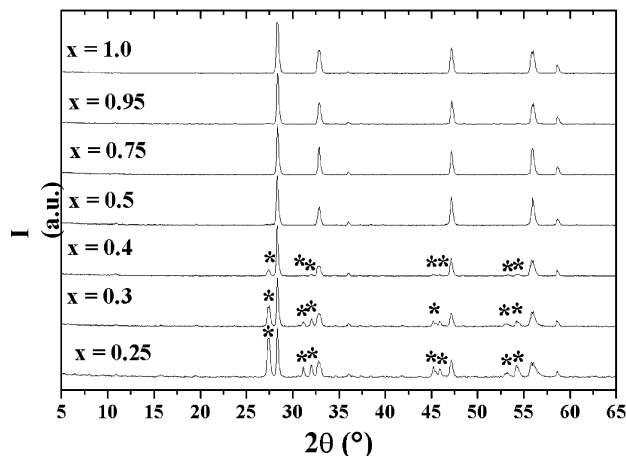


Figure 1. X-ray diffraction patterns of $\text{Bi}_2\text{O}_3:(1-x)\text{MoO}_3:x\text{WO}_3$ ($0 < x \leq 1$) after the last heating at 950°C (* – $\gamma(\text{H})\text{Bi}_2\text{MoO}_6$).

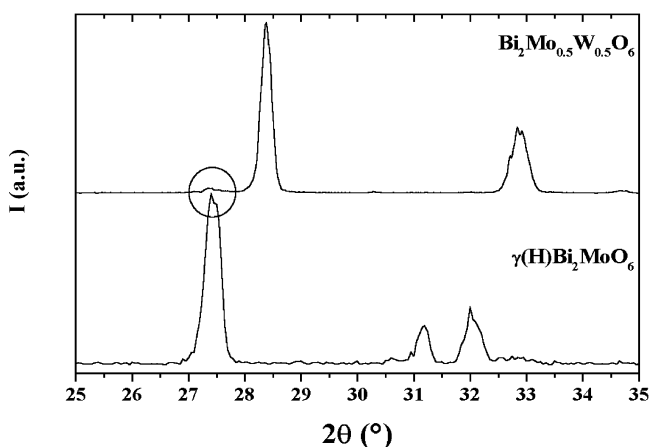


Figure 2. X-ray diffraction patterns of nominal composition $\text{Bi}_2\text{Mo}_{0.5}\text{W}_{0.5}\text{O}_6$ and $\gamma(\text{H})\text{Bi}_2\text{MoO}_6$ oxide.

als, representative compositions $x = 0.75$, as well as $x = 1$ for the sake of comparison, were prepared from mechanochemically activated precursors. This method has been applied successfully to the synthesis of several bismuth-layered ferroelectric materials,^{24–26} producing excellent results by improving the processing conditions and electrical properties of the ceramics.

TEM studies reveal that the mechanical treatment produces amorphous particles of 150–300 nm (Figure 3), with compositions always very close to the nominal $\text{Bi}_2\text{Mo}_{0.25}\text{W}_{0.75}\text{O}_6$, as EDS results show. This, together with the absence of any significant amount of crystals or particles of the starting oxides, is an indication of mechanosynthesis, i.e., synthesis induced exclusively by the mechanical treatment. Similar results were obtained for other Aurivillius oxides with $n = 1$, like $\text{Bi}_4\text{V}_2\text{O}_{11}$ or the parent Bi_2MoO_6 .²⁷ However, in the mixture of two oxides ($\text{Bi}_2\text{O}_3/0.5\text{V}_2\text{O}_5$ and $\text{Bi}_2\text{O}_3/\text{MoO}_3$) we were able to observe small crystallites of the final phase after mechanochemical activation. Most probably the energy

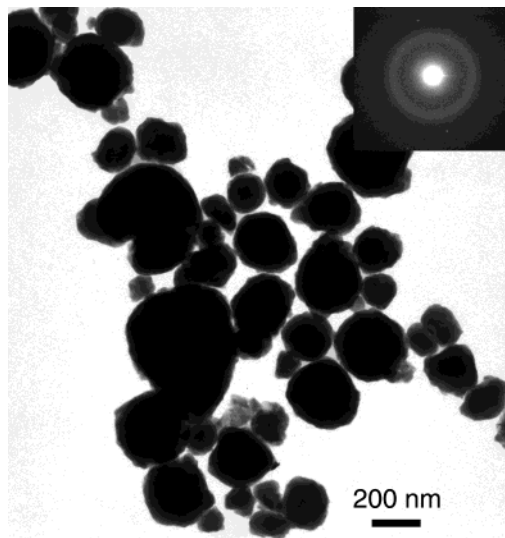


Figure 3. TEM micrograph of several particles from the mechanoactivated 1:0.25:0.75 $\text{Bi}_2\text{O}_3/\text{MoO}_3/\text{WO}_3$ mixture. The inset shows an electron diffraction pattern of the amorphous particles.

requirements for the formation of the complex oxide from three components (1:0.25:0.75 $\text{Bi}_2\text{O}_3/\text{MoO}_3/\text{WO}_3$) are higher, and, for the same milling conditions, the formation of crystallites is not reached in this case.

To study the crystallization process of the $\text{Bi}_2\text{Mo}_{1-x}\text{W}_x\text{O}_6$ phases from the mechanically activated amorphous precursors, their thermal behavior was studied by thermogravimetric and differential thermal analysis, as well as by X-ray powder diffraction at increasing temperatures. TG analyses confirm that no weight change is observed between room temperature and 1000°C . In contrast, the DTA tracings (Figure 4) show the existence of two exothermic processes on heating, centered at 410 and 470°C and 425 and 449°C for Bi_2WO_6 and $\text{Bi}_2\text{Mo}_{0.25}\text{W}_{0.75}\text{O}_6$, respectively. The X-ray diffraction patterns recorded at higher temperatures (Figure 5) confirm the formation of one well defined and very crystalline Aurivillius-type phase in the temperature range observed in DTA. The existence of two peaks can be attributed to the formation of an intermediate fluorite-like phase before the crystallization of the Aurivillius oxide, similarly to that reported for other related oxides such as Bi_2MoO_6 ,^{6,7} $\text{Bi}_3\text{TiNbO}_9$,²⁴ and $\text{Bi}_4\text{Ti}_3\text{O}_{12}$.²⁸ Unfortunately, in the present cases the fluorite phases cannot be isolated because they transform to the final Aurivillius phase at a temperature very close to that of their formation.

Finally, the DTA tracings show the existence of one endothermic effect, on heating, at 939 and 904°C for Bi_2WO_6 and $\text{Bi}_2\text{Mo}_{0.25}\text{W}_{0.75}\text{O}_6$, respectively, which is reversible on cooling with a noticeable hysteresis. The corresponding exothermic peaks are centered at 845 and 813°C . These processes are attributed to a ferro-paraelectric transition. It is worth noting two facts: the 939°C value matches exactly the Curie temperature reported for Bi_2WO_6 ,¹⁰ and a similar reversible transition occurs in $\gamma(\text{L})\text{Bi}_2\text{MoO}_6$ at 607°C , due to the transformation $\gamma(\text{L})-\gamma(\text{I})\text{Bi}_2\text{MoO}_6$, that is, the ferro-paraelectric transition.⁶ Thus, it can be concluded that

(24) Castro, A.; Millán, P.; Pardo, L.; Jiménez, B. *J. Mater. Chem.* **1999**, *9*, 1313.

(25) Pardo, L.; Castro, A.; Millán, P.; Alemany, C.; Jiménez, R.; Jiménez, B. *Acta Mater.* **2000**, *48*, 2421.

(26) Moure, A.; Pardo, L.; Alemany, C.; Millán, P.; Castro, A. *J. Eur. Ceram. Soc.* **2001**, *21*, 1399.

(27) Ricote, J.; Pardo, L.; Castro, A.; Millán, P. *J. Solid State Chem.* **2001**, *160*, 54.

(28) Lisoni, J. G.; Millán, P.; Vila, E.; Martín de Vidales, J. L.; Hoffmann, Th.; Castro, A. *Chem. Mater.* **2001**, *13*, 2084.

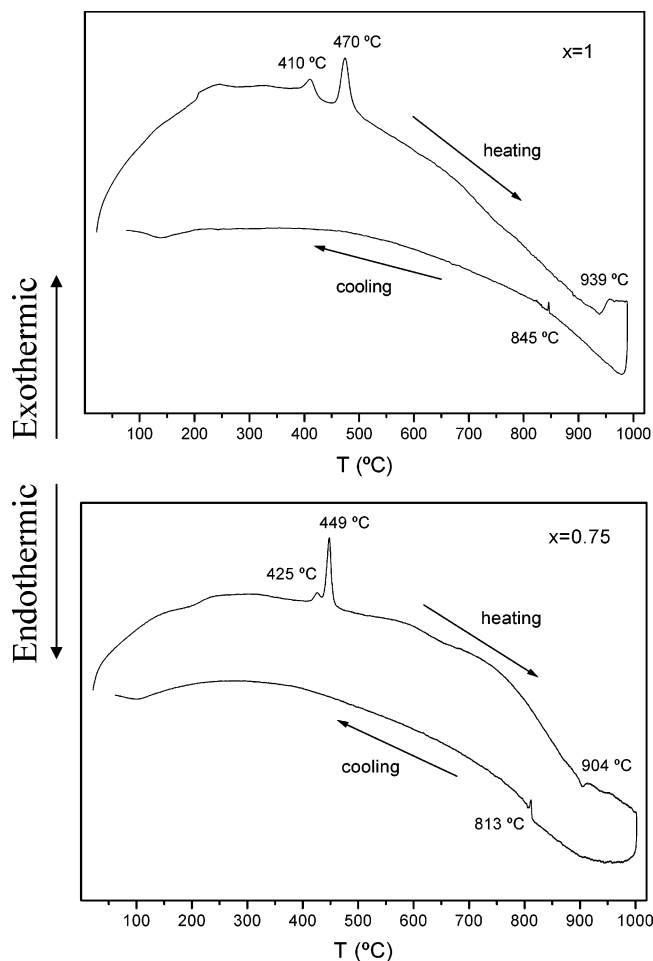


Figure 4. Differential thermal analysis of $\text{Bi}_2\text{O}_3:(1-x)\text{MoO}_3:x\text{WO}_3$ ($x = 0.75, 1$) amorphous powders (30 days of mechanical milling).

the substitution of molybdenum for tungsten in Bi_2WO_6 leads to a reduction of the Curie temperature.

To ascertain the true nature of the reversible endothermic–exothermic effect detected by thermal analysis, the electrical behavior of ceramics with the new $\text{Bi}_2\text{Mo}_{0.25}\text{W}_{0.75}\text{O}_6$ composition was studied.

The $\text{Bi}_2\text{Mo}_{0.25}\text{W}_{0.75}\text{O}_6$ ceramics were prepared from the mechanoactivated precursor powder, according to the protocol previously reported in the Experimental Section. The measurements of the dielectric constant versus temperature, carried out at 100 kHz (Figure 6), show a wide maximum and a narrow peak. The temperature corresponding to the wide maximum increases with the frequency of measurement, while that of the narrow peak is frequency independent, and occurs at 908 °C on heating, corresponding to the ferro–paraelectric phase-transition temperature of $\text{Bi}_2\text{Mo}_{0.25}\text{W}_{0.75}\text{O}_6$, and at 842 °C on cooling, so that a 66 °C thermal hysteresis takes place in the phase transition. These temperatures match very well those of the transition peaks observed by DTA.

From the room-temperature hysteresis loops (Figure 7) values of $3.8 \mu\text{C}\cdot\text{cm}^{-2}$ and $46 \text{ kV}\cdot\text{cm}^{-1}$ for remnant polarization and coercive field, respectively, were obtained.

Very well crystallized $\text{Bi}_2\text{Mo}_{0.25}\text{W}_{0.75}\text{O}_6$ powdered single phase, obtained by classical solid-state reaction, was used for the structural study of this oxide. Its

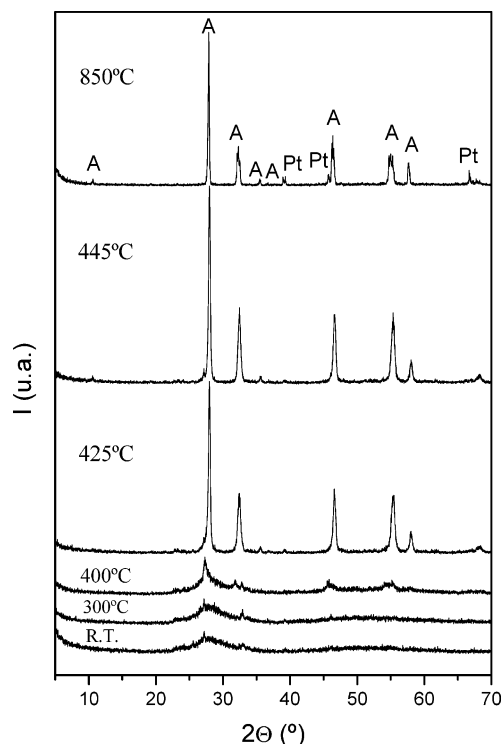


Figure 5. X-ray diffraction patterns at increasing temperatures of 1:0.25:0.75 $\text{Bi}_2\text{O}_3/\text{MoO}_3/\text{WO}_3$ amorphous powder (30 days of mechanical milling; Pt = platinum; A = Aurivillius-type phase).

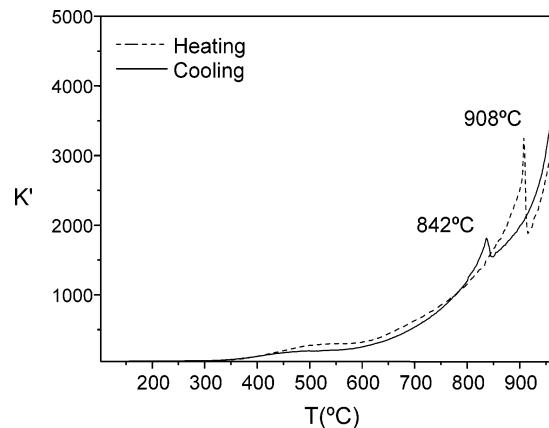


Figure 6. Dielectric constant as a function of the temperature, heating–cooling cycle, for the $\text{Bi}_2\text{Mo}_{0.25}\text{W}_{0.75}\text{O}_6$ at 100 kHz measuring frequency.

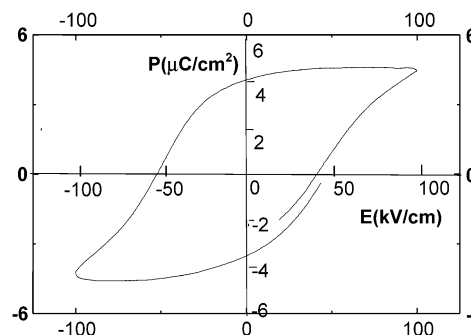


Figure 7. Room-temperature hysteresis loop at the frequency of 0.1 Hz for $\text{Bi}_2\text{Mo}_{0.25}\text{W}_{0.75}\text{O}_6$ material.

powder diffraction pattern can be completely indexed on the basis of an orthorhombic cell with $a \approx 5.4 \text{ \AA}$, $b \approx 16.4 \text{ \AA}$, and $c \approx 5.5 \text{ \AA}$, belonging to space group $Pca2_1$.

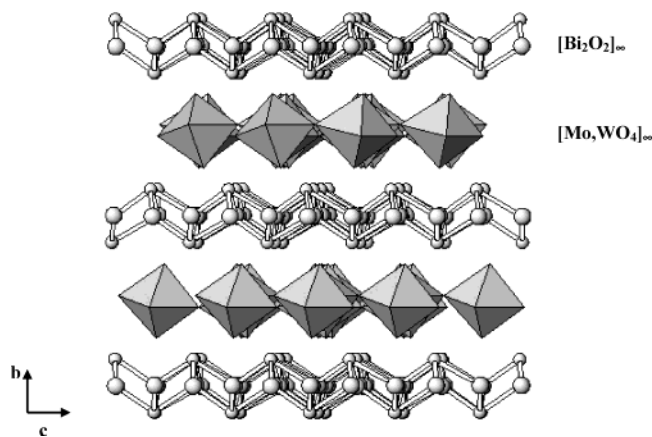


Figure 8. Projection of the $\text{Bi}_2\text{Mo}_{0.25}\text{W}_{0.75}\text{O}_6$ structure.

Table 1. Unit-Cell Parameters and Reliability Factors of the Rietveld Refinements of $\text{Bi}_2\text{Mo}_{0.25}\text{W}_{0.75}\text{O}_6$ Structure and the Isostructural Bi_2WO_6 and $\gamma(\text{L})\text{Bi}_2\text{MoO}_6$ Oxides^a

	X-ray, Cu K α	neutron, 1.910 Å	Bi_2WO_6 ¹⁶	$\gamma(\text{L})$ Bi_2MoO_6 ²⁹
a (Å)	5.4474(2)	5.44547(7)	5.4373(2)	5.4896(3)
b (Å)	16.3804(7)	16.3731(2)	16.4302(5)	16.2266(7)
c (Å)	5.4691(2)	5.46659(7)	5.4584(2)	5.5131(3)
V (Å ³)	488.01(4)	487.40(1)	487.63(5)	491.09(5)
ρ_{cal} (g·cm ⁻³)	9.20	9.21	9.50	9.44
χ^2	4.07	4.32		
R_p (%)	15.4	4.69	5.19	
R_{wp} (%)	20.1	6.64	5.94	
R_{Bragg} (%)	11.5	3.58		
R_F (%)	9.61	3.00	3.69	

^a Orthorhombic system, space group $Pca2_1$, $Z = 4$.

The refinement of the $\text{Bi}_2\text{Mo}_{0.25}\text{W}_{0.75}\text{O}_6$ structure (Figure 8) was undertaken starting from the structural model of the isostructural Bi_2WO_6 ¹⁶ oxide.

In the first stage, the X-ray diffraction data were used to refine the unit-cell parameters, the cation coordinates, and the occupancy parameters for the Mo/W site, which allowed a verification of the molybdenum/tungsten ratio. No attempt was made to refine the oxygen sites, and they were left fixed. In the final stage of the refinement a total of 24 parameters were varied freely including the coordinates of Bi atoms and the coordinates and occupation of Mo/W atoms. The background was computed with the usual polynomial function, and a pseudo-Voigt profile function was used for peak fitting. Final profile and Bragg agreement factors are reported in Table 1 together with the unit-cell parameters for this $\text{Bi}_2\text{Mo}_{0.25}\text{W}_{0.75}\text{O}_6$ oxide. The final refined coordinate values and occupation factors are

given in Table 2. Parameters given without the standard deviations were not refined.

Structural refinement from neutron data was carried out in the same way, except that the positional parameters of oxygen atoms and thermal parameters for all atoms were also refined during the last cycles, with a total of 51 fitted parameters. Results of this refinement are reported in Tables 1 and 2, and selected interatomic distances are presented in Table 3. The observed and calculated diffraction patterns are shown in Figure 9a for X-ray and in Figure 9b for neutron refinements, respectively.

Both structure refinements resulted in good agreement between experimental and calculated patterns as can be observed in Figure 9 and Table 1, with particularly good R values for neutron data (note the $R_{\text{Bragg}} = 3.58\%$). Because the refined atom positional parameters are rather similar in both cases, the discussion on the structure of $\text{Bi}_2\text{Mo}_{0.25}\text{W}_{0.75}\text{O}_6$ will be based on the neutron data analysis, which is certainly more reliable.

It is interesting to note that the value of Mo/W ratio of 0.21(2):0.79(2), obtained from the structural refinement, is very near the nominal starting composition 0.25:0.75.

The structure of $\text{Bi}_2\text{Mo}_{0.25}\text{W}_{0.75}\text{O}_6$ can be described in the same way as those of the parent Bi_2WO_6 ¹⁶ and $\gamma(\text{L})\text{Bi}_2\text{MoO}_6$ ^{15,29} phases. It is built up by the stacking of bismuth–oxygen $[\text{Bi}_2\text{O}_2]$ slabs and $[\text{Mo}/\text{WO}_4]$ layers, as represented in Figure 8. Such layers are constituted by molybdenum/tungsten–oxygen octahedra sharing all the equatorial corners. The unit-cell parameters are comprised between those of the Bi_2WO_6 and $\gamma(\text{L})\text{Bi}_2\text{MoO}_6$ (Table 1).

The coordination of bismuth atoms is little affected by molybdenum substitution in $\text{Bi}_2\text{Mo}_{0.25}\text{W}_{0.75}\text{O}_6$. The coordination polyhedra are very irregular, a general trend of cations possessing a lone pair of electrons, and, particularly, bismuth in Aurivillius-type phases. Both Bi1 and Bi2 are bonded to four oxygens of their layer at distances ranging from 2.161 to 2.530 Å, and to two other oxygens belonging to the apical corner of Mo/WO_6 octahedra, at distances ranging between 2.443 and 2.577 Å.

The molybdenum or tungsten atoms are randomly distributed in the $[\text{Mo}/\text{WO}_4]$ layers, surrounded by six oxygens in a quite distorted octahedral coordination. The Mo/W–O distances range from 1.765 to 2.197 Å. It is worth noting that the cations are displaced from the center of the octahedra by 0.27 Å, and that the magnitude of such displacement is very similar for Bi_2WO_6

Table 2. Fractional Atom Coordinates and Isotropic Thermal Displacement Parameters (Å²) in the Structure of $\text{Bi}_2\text{Mo}_{0.25}\text{W}_{0.75}\text{O}_6$ ^a

atom	X-ray, Cu K α				neutron, 1.910 Å			
	x	y	z	B	x	y	z	B
Bi1	0.521(1)	0.4213(6)	0.970(1)	0.27	0.5211(7)	0.4224(2)	0.980(1)	0.27(2)
Bi2	0.480(1)	0.0763(6)	0.983(1)	0.27	0.4824(6)	0.0779(2)	0.985(1)	0.27(2)
Mo/W	0.009(3)	0.249(1)	0	0.05	0.003(1)	0.2488(5)	0	0.05(6)
O1	0.063	0.140	0.081	0.67	0.063(2)	0.1399(7)	0.081(1)	0.67(5)
O2	0.260	0.999	0.270	0.31	0.2603(7)	0.9989(4)	0.270(1)	0.31(3)
O3	0.240	0.501	0.262	0.31	0.2399(7)	0.5011(4)	0.262(1)	0.31(3)
O4	0.704	0.232	0.257	0.45	0.704(1)	0.2317(3)	0.257(1)	0.45(4)
O5	0.210	0.264	0.342	0.45	0.210(1)	0.2637(4)	0.342(1)	0.45(4)
O6	0.554	0.359	0.571	0.67	0.554(1)	0.3593(6)	0.571(1)	0.67(5)

^a All atoms are placed in the general 4a Wyckoff sites; the occupation factor obtained for Mo/W is 0.21(2)/0.79(2).

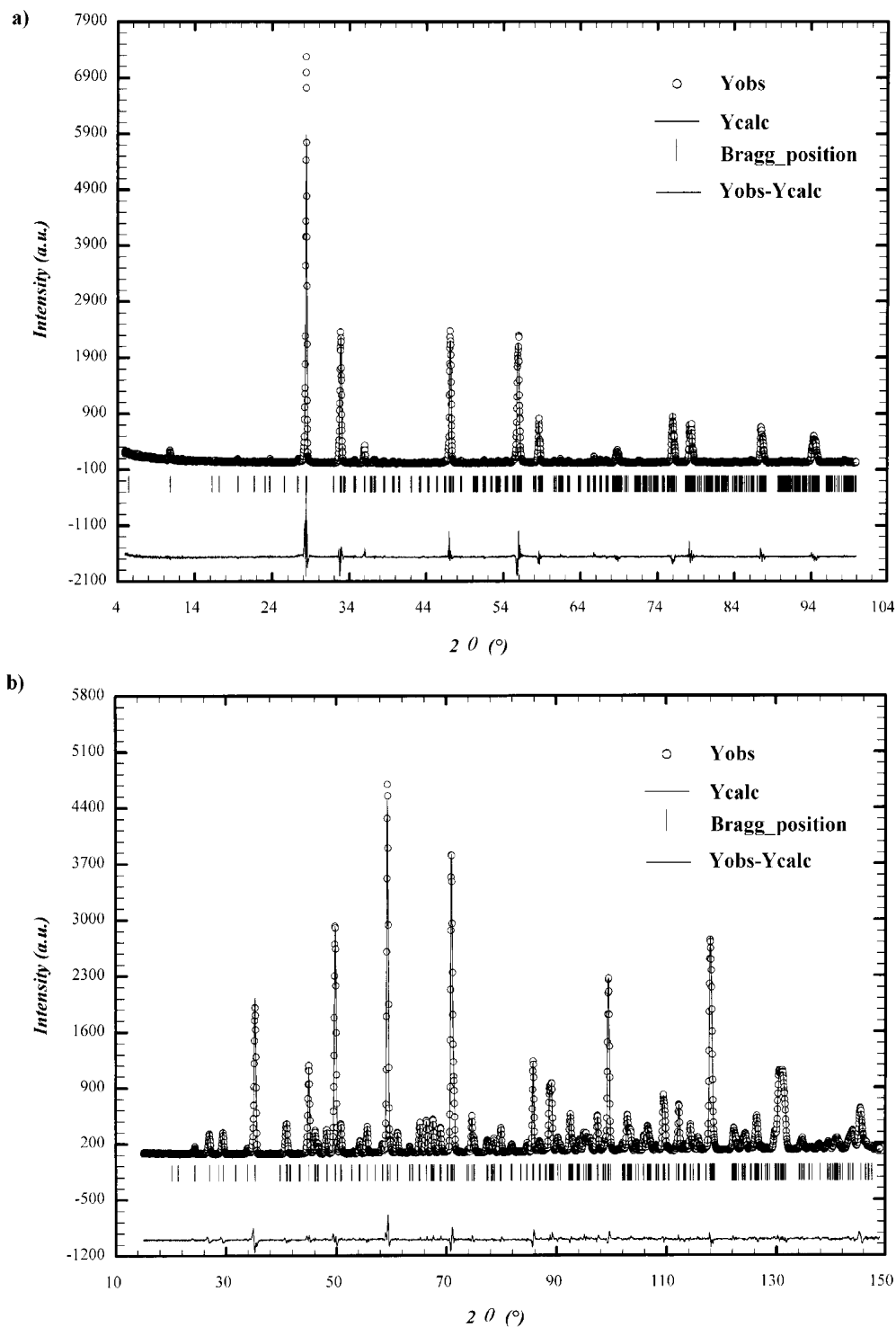


Figure 9. Observed (○), calculated (solid line), and difference (lower full line) diffraction patterns for $\text{Bi}_2\text{Mo}_{0.25}\text{W}_{0.75}\text{O}_6$ (a) X-ray and (b) neutron refinements. Vertical bars at the bottom indicate the Bragg positions.

(0.28 Å) and considerably higher for $\gamma(\text{L}) \text{Bi}_2\text{MoO}_6$ (0.36 Å). This fact is very important taking into account that the displacement vector of molybdenum or tungsten atoms away from the octahedron center is almost entirely in the polar axis direction of these materials,¹⁶ having a great influence on their ferroelectric properties.

Moreover, the equatorial planes of octahedra are tilted from the (010) plane in the three structures with

Table 3. Selected Bi–O and Mo/W–O Distances (Å) in the Structure of $\text{Bi}_2\text{Mo}_{0.25}\text{W}_{0.75}\text{O}_6$ from Neutron Data Rietveld Analysis (E.S.D. = 0.008 Å)

Bi1–O3	2.161	Bi2–O2	2.191	Mo/W–O4	1.765
Bi1–O3	2.262	Bi2–O2	2.219	Mo/W–O5	1.802
Bi1–O3	2.313	Bi2–O2	2.359	Mo/W–O1	1.866
Bi1–O6	2.469	Bi2–O1	2.443	Mo/W–O6	1.876
Bi1–O3	2.530	Bi2–O2	2.510	Mo/W–O4	2.169
Bi1–O6	2.577	Bi2–O1	2.554	Mo/W–O5	2.197

roughly the same values: 10.3° in $\gamma(\text{L}) \text{Bi}_2\text{MoO}_6$, 10.8° in Bi_2WO_6 , and 10.9° in $\text{Bi}_2\text{Mo}_{0.25}\text{W}_{0.75}\text{O}_6$ phases.

(29) Theobald, F.; Laarif, A.; Hewat, A. W. *Ferroelectrics* **1984**, *56*, 219.

In summary, the substitution of tungsten for molybdenum in $\gamma(\text{L}) \text{Bi}_2\text{MoO}_6$ keeps the structural framework of the Aurivillius-type structures, with characteristics midway between those of $\gamma(\text{L}) \text{Bi}_2\text{MoO}_6$ and Bi_2WO_6 , depending on the Mo/W ratio.

Acknowledgment. This work was funded by MAT2001-0561 (MCyT, Spain) and 07N/0076/2002 (CAM, Spain) projects. We are grateful to Institut Laue

Langevin (Grenoble, France) and to Universidad Carlos III (Madrid, Spain) for making all facilities available. We thank Prof. J. E. Iglesias (ICMM/CSIC, Spain) and Dr. M. T. Fernández-Díaz (ILL, France) for many fruitful discussions. Thanks are also given to Ms. M. Antón for preparation of the samples. P.B. thanks the Spanish Government for the grant awarded.

CM030224R